Earthquake Magnitudes Before and After the Mineral, Virginia Event

Christine Liu

Advisor: Dr. Laurent Montési

November 27, 2013

Geology 394

Table of Contents

List of Figures

List of Tables

Abstract

Intraplate earthquakes can occur in the interior of tectonic plates but are very rare. Similar to all earthquakes, they can generate changes in stress in the aftershock zone, near-fields, and at long distances of up to thousands of kilometers from their epicenters. The Mineral, Virginia intraplate earthquake that occurred on August 23, 2011 had an exceptionally high magnitude M_w = 5.8. Another exceptionally large earthquake occurred recently in the Indian Ocean with a magnitude of M_w= 8.6. This Indian Ocean earthquake was broadly felt over 10,000 km from the epicenter and triggered additional events worldwide. The research presented here was undertaken to determine if the Mineral earthquake may have had a similar effect to Indian Ocean event, namely, if the seismic activity of the Central and Eastern US (CEUS), throughout which shaking from the earthquake was felt, increased in the days and weeks following the earthquake.

Several methods can determine the statistical level of significance of the changes in seismicity. A frequency/magnitude diagram shows that the magnitude of completeness is around M_w = 2.0 of the ten years prior to the Mineral, Virginia earthquake. A statistical analysis of that time period is used to determine the expected seismic activity of the CEUS. Post-Mineral moment release rates did not exceed the 95 percentile of expected moment release rate, especially if the Mineral aftershock and two events for magnitude larger than 4.2 are removed from the catalogue. The same analysis applied to a high-quality catalogue focused on the New Madrid Seismic Zone returned similar conclusions. Therefore, it does not appear that the seismic moment release in the Mineral Earthquake increased significantly in the CEUS.

Introduction

Intraplate earthquakes occurring in the interior of tectonic plates are rare, and can result in significant damage (Stein, 2010). Like every earthquake, they can generate changes in stress in the aftershock zone, near-field, and at long distances of up to thousands of kilometers from their epicenters. One of the largest intraplate earthquakes to be recorded was in the lower 48 states, which was the 1811-1812 New Madrid earthquake events (Stein, 2010). New Madrid had four earthquakes with magnitudes ranging from $M_w = 7.2$ to $M_w = 8.1$ and was broadly felt over 2.5 million square kilometers (USGS, 2012).

A portion of the energy released by an earthquake can alter the state of stress and induce damage in regions that surround the earthquake source. The triggering of new earthquakes is the result from the change in state of stress. Velasco et al. (2008) classified the triggering of earthquakes into two categories: static and dynamic triggering.

Static triggering occurs within a few fault lengths of the mainshock rupture and results from changes in the local stress field induced by the earthquake slip (Velasco et al, 2008). Aftershocks are likely triggered by static triggering. Aftershocks occur after a large earthquake because the movement on the fault increases the stress, which acts on the fault itself and nearby. Parts of the fault slip more than others in the large earthquake causing a new pattern of stress in the fault. Aftershocks can be distinguished from the mainshock because of a distinctive decrease in activity over time and a distinctive distribution of magnitude. This stress change can also produce new mainshocks on nearby faults (Stein, 1999). One example is the 1992 Landers earthquake that is famous for having triggered the Big Bear earthquakes a few hours after, and the 1999 Hector Mine earthquake 20 km away (Freed et al., 2001).

Dynamic triggering is expressed by an increase in earthquake activity far away from the mainshock that correlates with the passage of Rayleigh and Love waves. These surface waves are large amplitude and long period seismic waves that travel along the surface of the Earth. Rayleigh waves are compressional and dilational as well as shearing, whereas Love waves only involve shearing (Velasco et al., 2008). Triggering by dynamic stresses can occur far from the mainshock because surface waves lose energy more slowly than static displacements. Dynamic stresses can also alter the mechanical state or properties of the fault zone, making them more likely to experience an earthquake in the near future (Kilb et al., 2000).

A recent earthquake in the Sumatra region demonstrates that triggering can occur by a third mechanism. Damage induced by dynamic stresses can reduce fault strength and increase seismicity even in regions very far from the mainshock (Pollitz et al., 2012).

The Indian Ocean earthquake took place on April 11, 2012. Due to its large magnitude of $M_w = 8.6$ and unusual shallow strike slip focal mechanism, this earthquake produced exceptionally high Love wave amplitude. It is estimated that shaking from this earthquake produced more ground shaking than any previously recorded earthquake (Pollitz et al., 2012). Increased seismicity was detected as far as 10,000-20,000 km from the mainshock. These triggered earthquakes were located along the four lobes of the Love-wave radiation pattern where high dynamic strain magnitudes are predicted (Pollitz et al, 2012). Shortly after, there were globally

five times more earthquakes during the six days following the main shock than would be expected from long term averages of seismicity (Figure 1) (Pollitz et al., 2012).

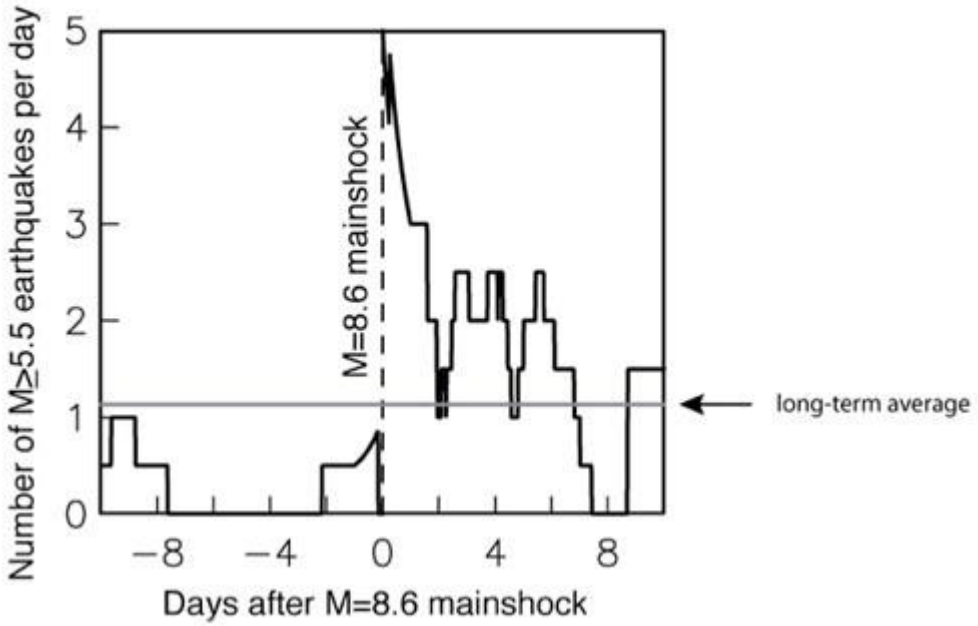

Figure 1. Number of earthquakes at least M_w=5.5 in the ten days preceding and ten days following the M_w = 8.6 mainshock in the Indian Ocean on April 11, 2012 compared with the long term average (Figure from Pollitz et al., 2012).

On August 23, 2011, Mineral, Virginia experienced a large, rare intraplate earthquake that shook a large region of the Central-Eastern United States. This earthquake event had an exceptionally high magnitude of M_w = 5.8 and resulted from a reverse fault slip on a Northeast striking plane (Figure 2A) within the Central Virginia Seismic Zone (CVSZ) (Horton et al, 2012). The reverse slip was caused by compressional forces where along the fault one block (hanging wall) was pushed up relative to the rock beneath the fault (foot wall) (Stein, 2010). The epicenter was located in the Chopawamsic Terrane of Piedmont, east of the Chopawamsic fault and west of the Spotsylvania fault (Fenster and Walsh, 2011). The CVSZ features a cluster of historic seismicity that is not associated with any known faults (Fenster and Walsh, 2011). The Mineral earthquake was the largest to shake the eastern United States since 1897 and was felt over an extraordinarily large area (Jibson and Harp, 2012). According to USGS, the event was felt along the eastern seaboard from Georgia to Northeastern Canada and west of Chicago (Horton et al, 2012). Figure 2C depicts the USGS "Did you feel it? "data map comparing two earthquakes on the eastern and western side of the United States with similar magnitudes and depth. The eastern region depicting the Mineral earthquake was felt more broadly than similar events in the western region of the US. The exceptional size and widespread ground shaking of the Mineral earthquake exhibits similarities with the 2012 Indian Ocean earthquake. Therefore, the Mineral event offers an opportunity to examine the role in static stress transfer, long- distance triggering, and aftershock decay following a moderate magnitude intraplate event.

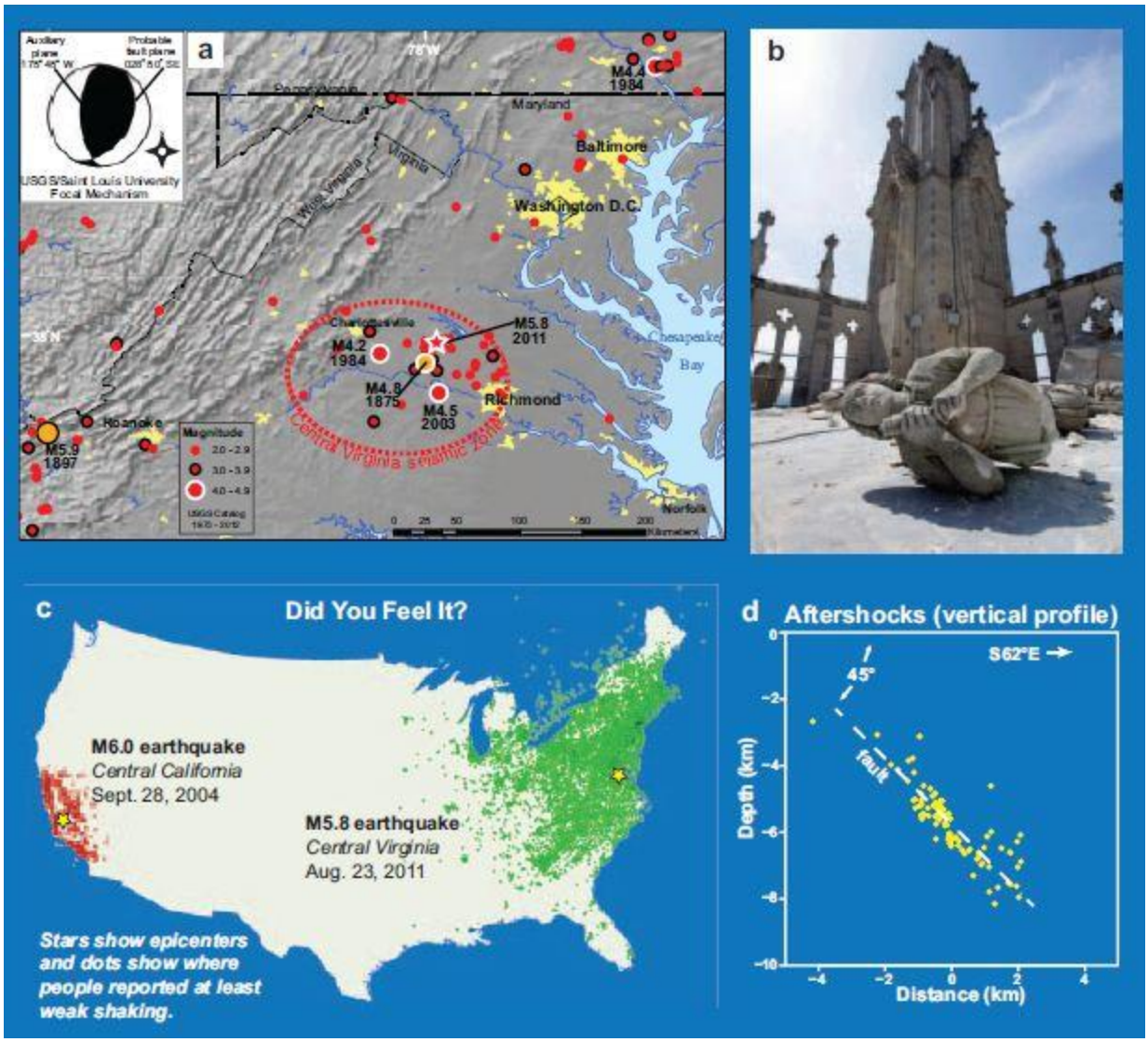

Figure 2. **(a)** M_w=5.8 earthquake in the Central Virginia Seismic zone with a focal plane indicating a reverse motion on an east-southeast dipping plane. **(b)** Damage to the Washington National Cathedral Building in Washington D.C., which was 135 km away from the epicenter. **(c)** USGS "Did You Feel It?" data map comparing earthquakes with similar magnitude and depth from the west region to the east region. The eastern region was felt broader than the western region. **(d)** The Virginia aftershocks were defined in an east-southeast dipping fault rupture plane. (Horton et al, 2012)

Shortly after the Mineral event, seismologists traveled to the epicenter region to deploy temporary seismic stations and have recorded over 200 aftershocks which enabled detailed delineation of the ruptured plane (Fenster and Walsh, 2011). Residents from Mineral, Virginia were experiencing aftershocks daily since the mainshock for an indefinite amount of time (Fenster and Walsh, 2011). USGS well monitoring recorded changes in groundwater levels in at least 48 wells that were located as far as 560 kilometers from the epicenter within minutes to 24 hours after the mainshock (Horton et al, 2012). Landslides triggered by the mainshock were observed 245 km away from the epicenter, indicating significant ground shaking over a large distance

(Jibson and Harp, 2012). This intense ground shaking may have damaged fault zones throughout eastern North America and triggered earthquakes.

Objectives of Research

A few months after the Mineral, Virginia event, a former graduate student, Lisa Walsh, noticed an increase in USGS earthquake alerts following the event (Walsh, personal communication, 2013). These alerts are triggered when an earthquake above a given magnitude is detected in a region of interest. Therefore, an increase in alerts could be due to an increase of earthquakes, or by generally larger earthquakes. This led us to investigate if the Mineral event may have a similar effect on the seismicity of eastern North America as the larger 2012 Indian Ocean earthquake had on the global seismicity.

Walsh had investigated as part of her PhD thesis if more earthquakes have occurred since the Mineral event than previously. Her results concluded that there was no significant difference in the number of earthquakes before and after the Mineral event (Walsh, personal communication, 2013). Therefore, the perceived increase of alerts may be due to an increased magnitude of earthquake that take place in the CEUS following the Mineral earthquake. My project consists of a statistical analysis of pre-Mineral seismicity to search for evidence of anomalous seismicity following the event.

Hypothesis

The earthquakes that have occurred since the Mineral event are generally larger than before the event. I hypothesize that the earthquakes that took place after the Mineral event would be anomalously large if the moment release rate after the Mineral event was larger than 95% of the time periods preceding the event.

Method of Analysis

I. Data Collection

To statistically analyze the seismicity data, an earthquake catalogue was collected from the publically available catalogue maintained by the Incorporated Research Institutions for Seismology (IRIS). After definition of a region and time span of interest, I downloaded a catalogue of events in a 'weed.event' file. The earthquake catalogue comprises time, date, magnitude, depth, and location of each individual event. The selected time span to characterize the pre-Mineral activity was January 01, 2001 to August 22, 2011. Post-Mineral activity was studied over at most 100 days following the mainshock. The region considered was the Central-Eastern United States. The location of this region is latitude 26.002 N to 46.769 N and longitude -94.529 W to -64.002 W (Figure 3).

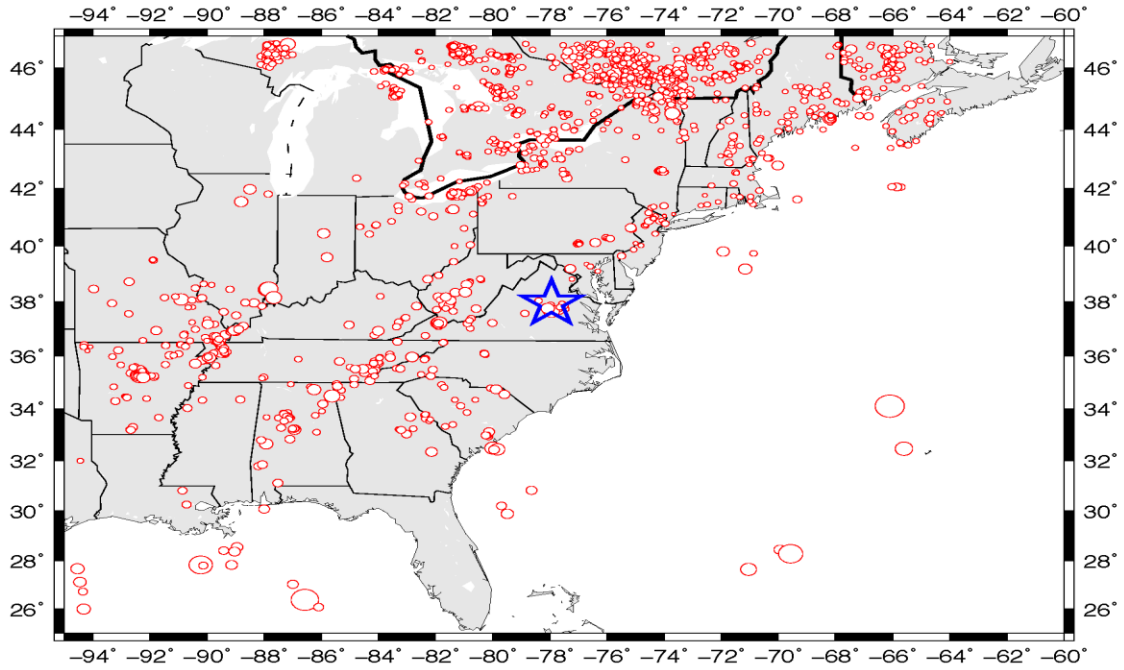

Figure 3. Map of the Central Eastern United States. Data was collected from IRIS and plotted using a Generic Mapping Tool (GMT). The blue star denotes the Mineral, Virginia earthquake.

The 'weed.event' file was parsed in Matlab rendering a 'textread' function. All of the information from the earthquake catalogue is stored into a structural array bookcase labeled 'Seis'. Each earthquake data corresponds to a cell in the array. The information associated with the cell includes latitude, longitude, depth, magnitude, date, time, reporting organization, and other information provided by the catalogue.

For each event, two derived data were determined. The reported time and date was converted into a serial date number using the Matlab function 'datenum' to avoid difficulties in handling variable month and year durations during the catalogue. The reported magnitude was converted into seismic moment using the Kanamori equation:

$$\mathrm{Mo} = 10^{\left(\left(\frac{3}{2}\right)\mathrm{Mw} + 9.1\right)} \qquad \text{Eq. 1}$$

where Mo is seismic moment and M_w is the reported moment magnitude. The Kanamori relation indicates that for each increase in magnitude by one unit, the moment and energy in the earthquake increases by a factor of roughly 30.

II. Gutenberg-Richter relation

The Gutenberg-Richter relation, or frequency-magnitude plot, describes the relation between number of earthquakes in a catalogue and their magnitude. Seismicity typically obeys a power law scaling relation, the Gutenberg-Richter relation, given by:

$$\log_{10} N = a - b\mathrm{M} \qquad \text{Eq. 2}$$

where *N* is the number of earthquakes with magnitudes larger than a magnitude M in the catalogue. The parameters *a* and *b* are constants where α depends on the time span and size of earthquake catalogue and *b* is the slope in the frequency-magnitude plot that is often close to 1. The parameters *a* and *b* are determined by conducting least square fits over a variety of magnitude intervals spanning at least one order of magnitude. This relation is best observed when the logarithm of the rate of earthquakes on the y-axis is plotted against the magnitude on the x-axis and forms a linear array. The slope of the line fits through the array and is extended to estimate how often a large earthquake may be expected in a period of time. A deviation from the Gutenberg-Richter relation at small magnitude is used to define the magnitude of completeness that is the smallest earthquake that can be assumed with high confidence is not missing in the dataset. Earthquakes that are smaller than the magnitude of completeness may not be detected or included in the catalogue. The magnitude of completeness is determined as the magnitude for which the parameter *b* changes from values close to 1 to values closer to 0.

III. Time Series with Moving Time Window

The time series plots individual calculated seismic moments for every date an event that occurred and can be used for examining average moment release rate within a certain time frame. The time series expresses the date on the x-axis and the seismic moment on the y-axis. The plot that was generated shows the history of seismicity during the time span of the catalogue. Since each event is a point without duration, there is no possibility to define a moment release rate for each individual event.

To define the moment release rate, the moving time window is used to smooth out the time series and remove some of the noise related to the randomness of individual events. The moment release rate Mr is calculated by the sum of the moments occurring within is time window divided by variable number of days in the window, L:

$$\mathrm{Mr} = \frac{1}{\mathrm{L}} \sum_{\mathrm{d}}^{\mathrm{d+L}} Mo \qquad \text{Eq. 3}$$

where d is the first day of the window. The window size considered is 10 days, 30 days, and 100 days.

In practice, the moving window averaging scheme determines what earthquakes took place between a start day d and a final d+L using the Matlab "find" function. Then it calculates the average of the moment of these earthquakes within that time frame. The process is repeated for the next "start day" and will continue until the "end day" reaches the end of the moments in the time series plot. Then the averaging scheme restarts for a different time window size. The moment release rate is plotted within the time series plot to show the average of the energy released from the earthquake source depending on the length of time.

IV. Cumulative Histogram

The moment release rates determined for each window size for the ten years preceding the Mineral event are analyzed by producing a cumulative histogram. The cumulative histogram is expressed as the log of the Moment Release Rates on the x-axis and the cumulative frequency on the y-axis. The cumulative frequency is the percentage of days for which the moment release is less than the associated moment release rate. The moment release rates for each window size are sorted. The 25^{th} percentile, median, and 75^{th} percentile of each moment release rate dataset are reported.

To examine the changes in seismicity rates, the post-Mineral moment release rate are compared with empirical statistical distribution of moment release rate determine in the pre-Mineral dataset. Earthquakes with magnitudes less than the magnitude of completeness are removed from the catalog. The average moment release rate over a period of time following the Mineral earthquake is calculated by taking the sum of the seismic moments and dividing it by the length of time considered. When collecting the post-Mineral data for the 10 day, the duration considered is August 24, 2011 to September 2, 2011. The seismic moments within that 10 day duration was summed up and divided by the 10 day length of time. This method is applied to the 30 and 100 day post-Mineral data. The duration for the 30 day is August 24, 2011 to September 22, 2011. The seismic moments contained within the 30 day duration are summed up and divided by 30 days. The duration for the 100 day is August 24, 2011 to December 1, 2011. The seismic moments contained within the 100 days are summed up and divided by 100 days.

The data from the post-Mineral period was collected from the IRIS catalogue containing the aftershocks. Aftershocks were identified based on a catalogue compiled by Dr. McNamara (US Geological Survey, Golden) available at ftp://ftpext.cr.usgs.gov/pub/cr/co/golden/mcnamara/ (database provided by Dr. Walsh). Post-Mineral moment release rate was re-calculated without the aftershock for an alternative view of the post-Mineral activity.

Results

Gutenberg – Richter Relation

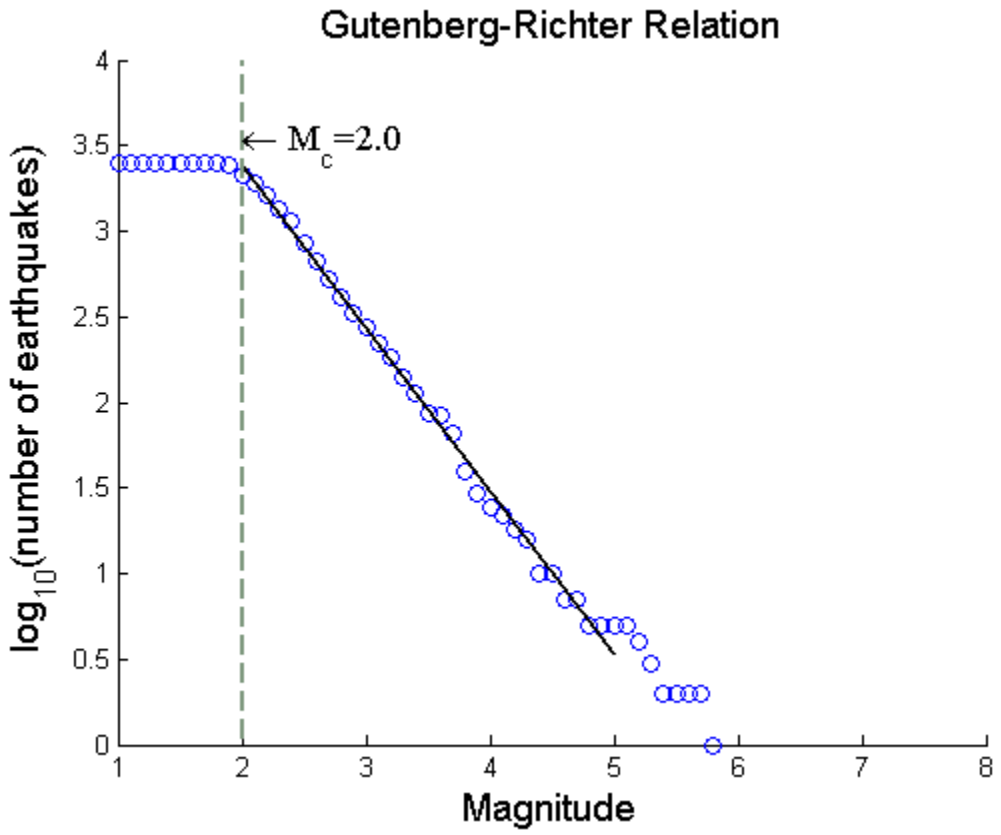

Figure 4. Gutenberg-Richter Relation Plot

In the Gutenberg-Richter plot (Figure 4), the magnitude of completeness is around M_C = 2.0. Earthquakes smaller than M_C = 2.0 are not detected systematically. Therefore they are included in the catalogue. The dataset collected from IRIS contains more than 2500 events over the ten years, which provides a representation of the pre-Mineral activity over 10 years. The *b* value forms a linear fit over the 2.0≤M≤5.8 range. To examine the changes in seismicity rate, all magnitudes below M_w= 2.0 were cut out of the catalogue.

Moving Time Windows

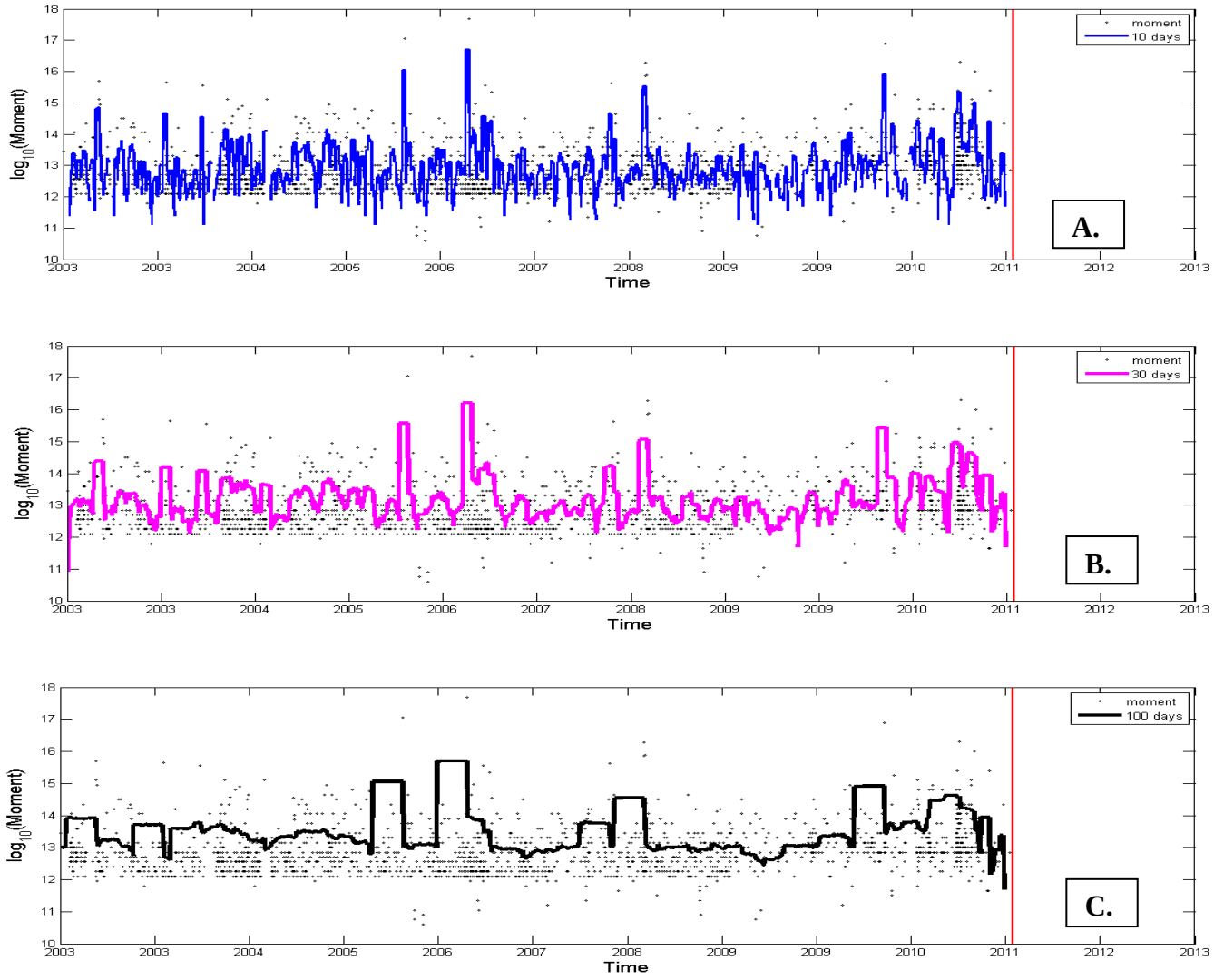

Figures 5. Seismic Moments and window moving averages in ten year duration prior to the Mineral, Virginia Event. The red line denotes the break before the Mineral Event. **A.** is the 10 day moving time window. **B.** is the 30 day time window. **C.** is the 100 day time window.

The 10 day, 30 day, and 100 day moving window averages have been calculated and plotted within the time series (Figure 5). The plot shows seismic moments and the window moving averages in the ten year duration before the Mineral event. The time series are very noisy for the 10 day and 30 day average. The 100 day average appears to be dominated by occasional large earthquakes.

Cumulative Histogram

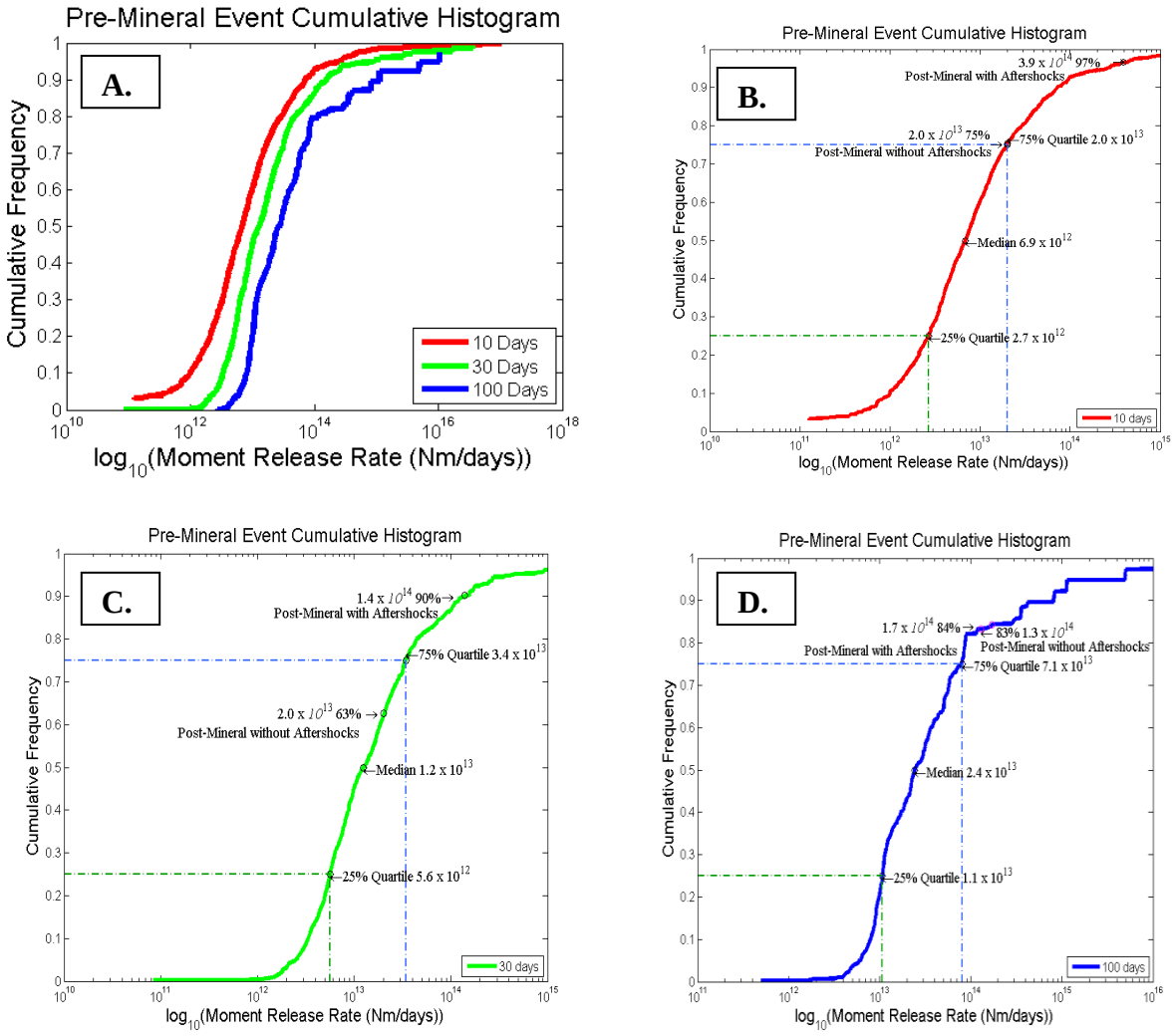

Figure 6. Cumulative Histograms of the Pre-Mineral Event with the Post-Mineral results with and without aftershocks extracted in three individual times. **A.** shows all of the moment release rates associated with the window sizes before separating them. **B.** shows the 10 day moment release rate with the inter-quartile range and the post-Mineral results with and without the aftershocks. **C.** shows the similarity with figure B on a 30 day moment release rate. **D.** shows the similarity with figure B and C on a 100 day moment release rate.

The cumulative histogram shows the distribution of moment release rate during the 10 years preceding the Mineral earthquake (Figure 6). The inter-quartile ranges for each of the moving time window averages of the pre-Mineral event are reported on the cumulative histograms (Figure 6) and on Table 1. All the plots show that the moment release rates in the 75th percentile were five times greater than the median, and the median was three times greater than the 25th percentile. The data is heavily skewed towards the larger moment release rates. The post-Mineral moment release rate was calculated and presented along with the pre-Mineral results to show if the post-Mineral results exceed the 95%.

The post-Mineral activity, including aftershocks did exceed 95% when average over 10 days. However the activity over 30 or 100 days following the event did not exceed the moment release rate (MRR) observed over 95% to the time in the 10 years preceding the event. The 10 day MRR was 3.9x 10^{14} Nm/Days (97% percentile), the 30 day MRR was 1.4x 10^{14} Nm/days (90% percentile), and the 100 day MRR was 1.7x10^{14} Nm/days (84% percentile). In the catalogue of the post-Mineral containing the aftershocks, there were three magnitudes of M_w= 3.4, M_w= 4.4, and M_w= 4.5 within the first ten days following the mainshock, which explained why the MRR is initially so high. These aftershocks were triggered by the Mineral event mainshock.

The post-Mineral catalogue with the aftershocks removed had lower MRR than the post-Mineral with the aftershocks contained. MRR no longer exceeds that observed 90% of the time during the 10 years preceding the Mineral event. The 10 day MRR were 2.0x10^{13} Nm/days (75% percentile), the 30 day MRR was 2.0x10^{13} Nm/days (63% percentile), and the 100 day MRR was 1.3x10^{14} Nm/days (83% percentile). The post-Mineral results with the aftershocks removed did not exceed beyond 83%. Therefore, it is clear that we do not see evidence in the CEUS IRIS catalogue for large magnitude earthquakes triggered by the Mineral earthquake outside of the aftershock zone.

MRR was also calculated with other window sizes ranging from 20 day to 90 days in order to show how the aftershocks have an effect at different times (Figure 7). The post-Mineral results with the aftershocks showed steady aftershock decay in the first 40 days and then a jump at 50 days. After 50 days, the moment release rate again decreases progressively. The post-Mineral results with the aftershocks removed showed variability within the first 40 days. MRR increases suddenly 50 days and decreases progressively afterward. The origin of the jump at 50 days was investigated and it was found that two large seismic events with magnitudes of M_w= 4.4 and M_w= 4.5 occurred east of North and South Carolina on the Atlantic Ocean on October 3, 2011. These unusual events dominate over the seismic moment release following the Mineral earthquake. These two seismic events were removed from the post-Mineral catalogue. MRR was recalculated with and without the aftershocks to examine if there is an effect on the seismicity rates during 50 days after the Mineral event. The results are displayed in Figure 7 and Table 1.

Table 1. Comparison of the post-Mineral with the pre-Mineral Moment Release Rates (MRR)

Central Eastern US Seismicity Comparison										
	10 Days	**20 Days**	**30 Days**	**40 Days**	**50 Days**	**60 Days**	**70 Days**	**80 Days**	**90 Days**	**100 Days**
1st Quartile (Nm/Days)	$2.7x10^{12}$	$4.4x10^{12}$	$5.6x10^{12}$	$6.6x10^{12}$	$7.5x10^{12}$	$8.7x10^{12}$	$9.6x10^{12}$	$1.0x10^{13}$	$1.0x10^{13}$	$1.1x10^{13}$
Median (Nm/Days)	$6.9x10^{12}$	$9.8x10^{12}$	$1.2x10^{13}$	$1.5x10^{13}$	$1.6x10^{13}$	$1.7x10^{13}$	$1.9x10^{13}$	$2.2x10^{13}$	$2.4x10^{13}$	$2.4x10^{13}$
3rd Quartile (Nm/Days)	$2.0x10^{13}$	$3.0x10^{13}$	$3.4x10^{13}$	$4.1x10^{13}$	$5.1x10^{13}$	$5.6x10^{13}$	$5.6x10^{13}$	$6.4x10^{13}$	$6.5x10^{13}$	$7.1x10^{13}$
Post-Mineral w/aftershocks (Nm/Days)	$3.9x10^{14}$	$2.0x10^{14}$	$1.4x10^{14}$	$1.1x10^{14}$	$3.4x10^{14}$	$2.8x10^{14}$	$2.4x10^{14}$	$2.1x10^{14}$	$1.9x10^{14}$	$1.7x10^{14}$
Post-Mineral w/aftershocks (%)	97%	93%	90%	86%	92%	91%	89%	88%	86%	84%
Post-Mineral w/o aftershocks (Nm/Days)	$2.0x10^{13}$	$1.1x10^{13}$	$2.0x10^{13}$	$1.6x10^{13}$	$2.6x10^{14}$	$2.2x10^{14}$	$1.9x10^{14}$	$1.6x10^{14}$	$1.5x10^{14}$	$1.3x10^{14}$
Post-Mineral w/o aftershocks (%)	75%	52%	63%	52%	91%	90%	88%	86%	85%	83%
Post-Mineral w/aftershocks (Nm/Days) two events removed	$3.9x10^{14}$	$2.0x10^{14}$	$1.4x10^{14}$	$1.1x10^{14}$	$9.4x10^{13}$	$7.9x10^{13}$	$6.9x10^{13}$	$6.1x10^{13}$	$5.4x10^{13}$	$4.9x10^{13}$
Post-Mineral w/aftershocks (%) two events removed	97%	93%	90%	86%	83%	79%	76%	73%	69%	65%
Post-Mineral w/o aftershocks (Nm/Days) two events removed	$2.0x10^{13}$	$1.1x10^{13}$	$2.0x10^{13}$	$1.6x10^{13}$	$1.9x10^{13}$	$1.7x10^{13}$	$1.5x10^{13}$	$1.4x10^{13}$	$1.3x10^{13}$	$1.1x10^{13}$
Post-Mineral w/o aftershocks (%) two events removed	75%	52%	63%	52%	55%	50%	45%	40%	36%	30%

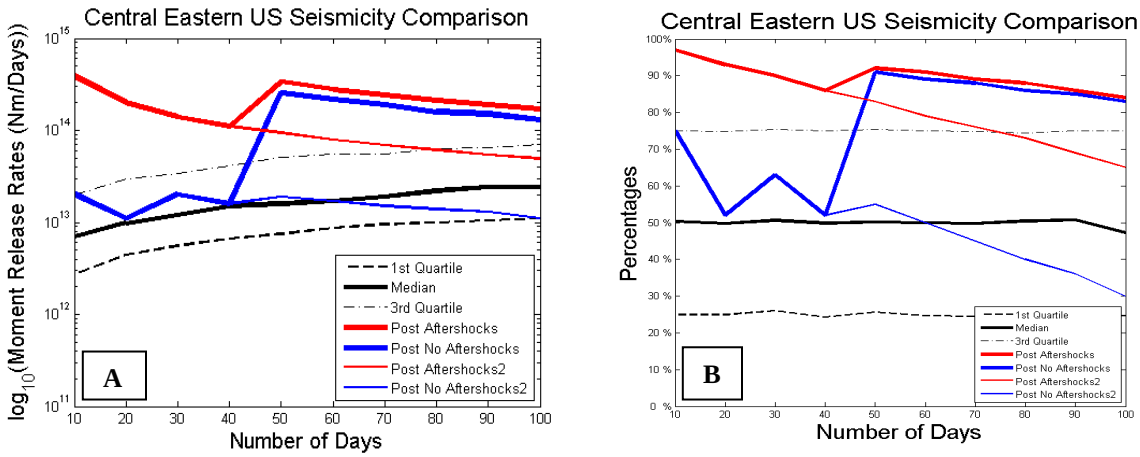

Figure 7. Two plots showing the post-Mineral data over the inter-quartile range with and without the aftershocks and two seismic events on a 100 days period. **A.** Plot shows the log of the MRR versus the 100 Days length of time to express the variability in the data of aftershock decay and two large seismic events. **B.** Percentages of the post-Mineral data over the 100 days length of time to express the variability in the data of the two events and aftershock decay.

In Figure 7 the plots show the seismicity comparisons between the Post-Mineral event with and without the aftershocks in the red and blue color. The black lines on both plots indicate the inter-quartile ranges. The two large seismic events were removed from the post-Mineral catalogue to perform a comparison of the one that contained aftershocks and the one with the aftershocks removed. The red line on both plots shows the post-Mineral results with the aftershocks included. The heavy red line includes the two large events and presents a jump at 50 days then later shows a steady decrease. The thin red line has the two seismic events removed and shows steady aftershock decay with no variability. The blue line on both plots shows the post-Mineral results with the aftershocks removed. The heavy blue line includes the two large events and shows noise within 40 days and a large jump at 50 days with a steady decrease. The thin blue line with the two events removed shows noise within the 40 days and then steady decay.

Removing the two Atlantic Ocean events removes the sudden jump in seismic release rate after 50 days. The post-Mineral catalogue without the aftershocks and two events removed showed some variability but a fairly constant moment release rate following the Mineral earthquake (Figure 7A). However, the percentile corresponding to this MRR decreases progressively, showing that the pre-Mineral data is dominated by occasional large events like the 10/03/2011 Atlantic Ocean events. There is no evidence that these large events or any of the post-Mineral activity except for aftershock is incompatible with the expectations from the pre-Mineral activity.

Two analyses were conducted to determine how frequently large magnitudes events would be expected to occur. The first analysis was using the Gutenberg-Richter plot to determine how often a seismic event of magnitude M_w= 4.4 or larger would occur in a year and when would that next seismic event be expected to occur. The Gutenberg-Richter plot indicates that 12.6 earthquakes of magnitude M_w= 4.4 or larger event took place during the 10 years of the catalog. Therefore, 1.3 earthquakes of magnitude of M_w=4.4 are expected to occur in a year, or equivalently one earthquake every 0.79 years (9.5 months or 288.5 days). The October 3rd events

took place only 39 days after the previous magnitude 4.4 or larger earthquake, which is early. However, this analysis does not take into consideration the natural variability of seismic activity.

The second analysis uses a compilation of the time intervals separating successive large earthquakes over the approximately ten year period from January 01, 2001 to the Mineral event to assess the variability of occurrence of these large earthquakes. For this analysis, a large earthquake is defined as having a magnitude in excess of M_w=4.3. Within that time range, there were 11 seismic events with magnitudes $\geq$ 4.3. Two of the large seismic events occurred on the same day. The ten time intervals before the Mineral event were sorted from least to greatest and plotted as a cumulative frequency diagram (Figure 8). The frequencies of the earthquake magnitudes $M_w \geq 4.3$ are centered around 100 days from over 30% to less than 60%. A statistical analysis was performed and the result was the 75th percentile was three times greater than the median, and the median was three times the 25th percentile. The time interval preceding the October 03, 2011 events was compared to this cumulative frequency diagram to determine how likely it is that these events occurred on that day based on the pre-Mineral activity red star on (Figure 8). The time interval for the post-Mineral event began on August 25, 2011 (aftershock magnitude M_w=4.5) and ended on October 3rd, 2011 (39 days). The time interval before the October 03, 2011 events is shorter than 22% of the pre-Mineral interval. Therefore, there is no indication that this event was exceptionally early (outside to the 1st and 3rd quartile of the pre-Mineral distribution). Figure (8) expresses the cumulative frequency on the y-axis and the number of days on the x-axis.

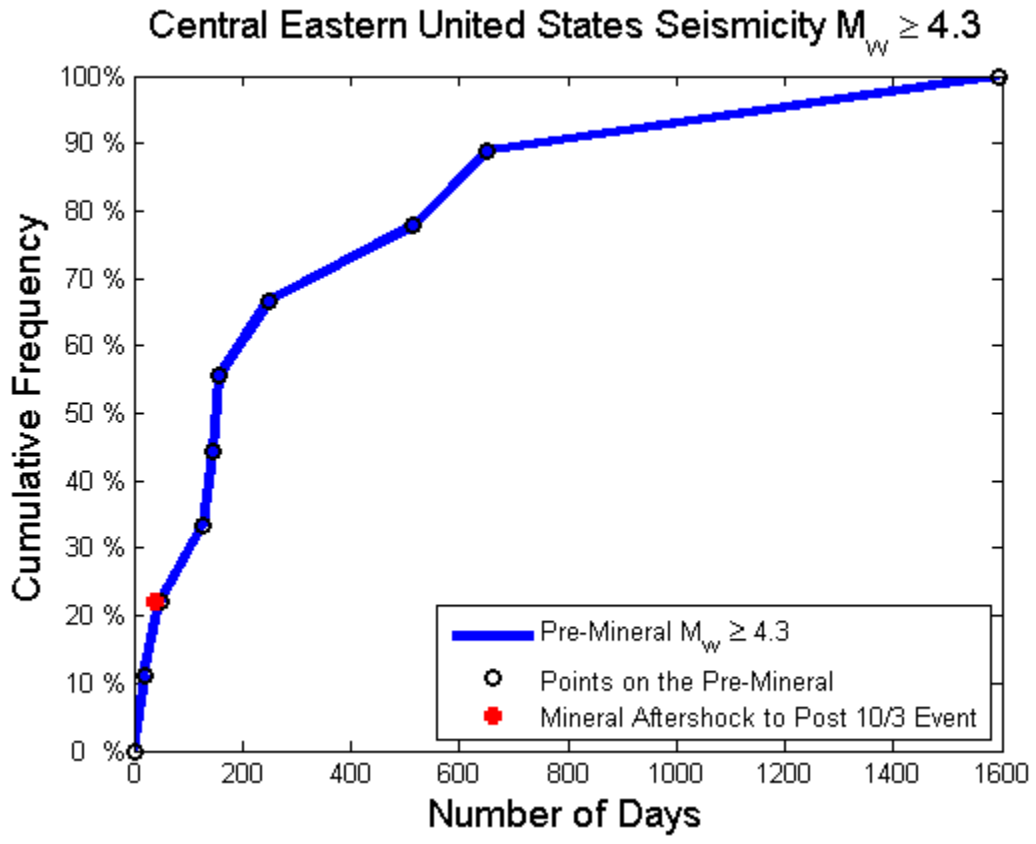

Figure 8. Plot of Mineral seismicity with $M_w \geq 4.3$ over a 10 year period on a cumulative frequency.

New Madrid Seismic Zone

When observing the catalogue of the Central Eastern United States, there are certain regions in the catalogue that have their own active seismicity. Changes in seismic activity that take place within one of these regions may not be apparent when studying the entire catalogue. In addition, scientific interest in these high activity regions may motivate installing a high quality local network of seismic stations that make it possible to capture more local earthquakes and reduce the magnitude of completeness.

The New Madrid Seismic Zone is an example of a well-known intraplate earthquake region. The purpose of examining the New Madrid Seismic zone is to investigate if the seismicities in this region were affected by the Mineral, Virginia Event. The methods that were performed in the Mineral earthquake event are applied to the detailed dataset focused on the New Madrid Seismic Zone.

Data Collection

The event catalogue was provided by the Center for Earthquake Research and Information (CERI) online browser (Figure 9). This earthquake browser contains seismicity data pertaining to information on the New Madrid Seismic Zone. The time chosen started at January 01, 2003 and went to August 22, 2011, including time preceding the Mineral event and 100 days after the event. The location of the New Madrid Seismic Zone that is focused on is Latitude (35N to 37N) and Longitude (-91 W to -88W). Only the last 8 years of data were chose because the seismic network was significantly improved in 2003. Therefore we only consider this span of time during which the seismic network was relatively stable so that detection thresholds, in particular, do not change over the time scale considered.

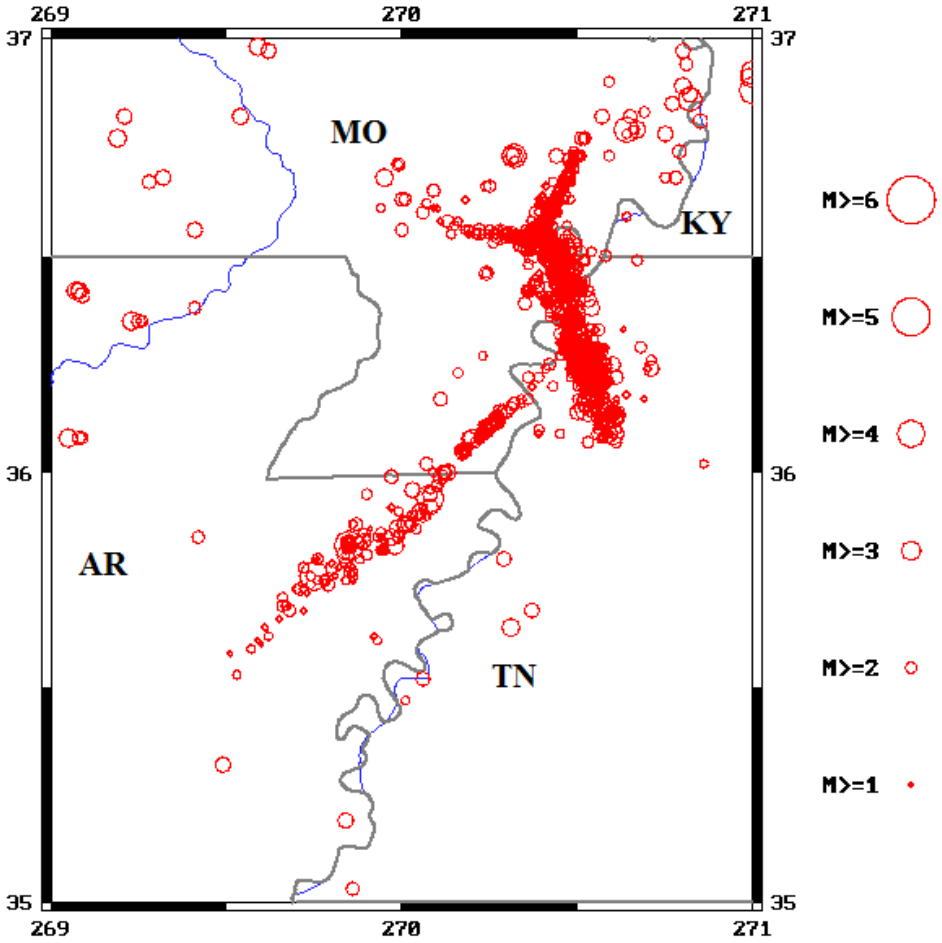

Figure 9. Map of the area concentrated on the New Madrid Seismic Zone. The plot shows seismicity collected eight years preceding the Mineral event. This map is available by Center for Earthquake and Research Information (CERI).

Gutenberg-Richter Relation

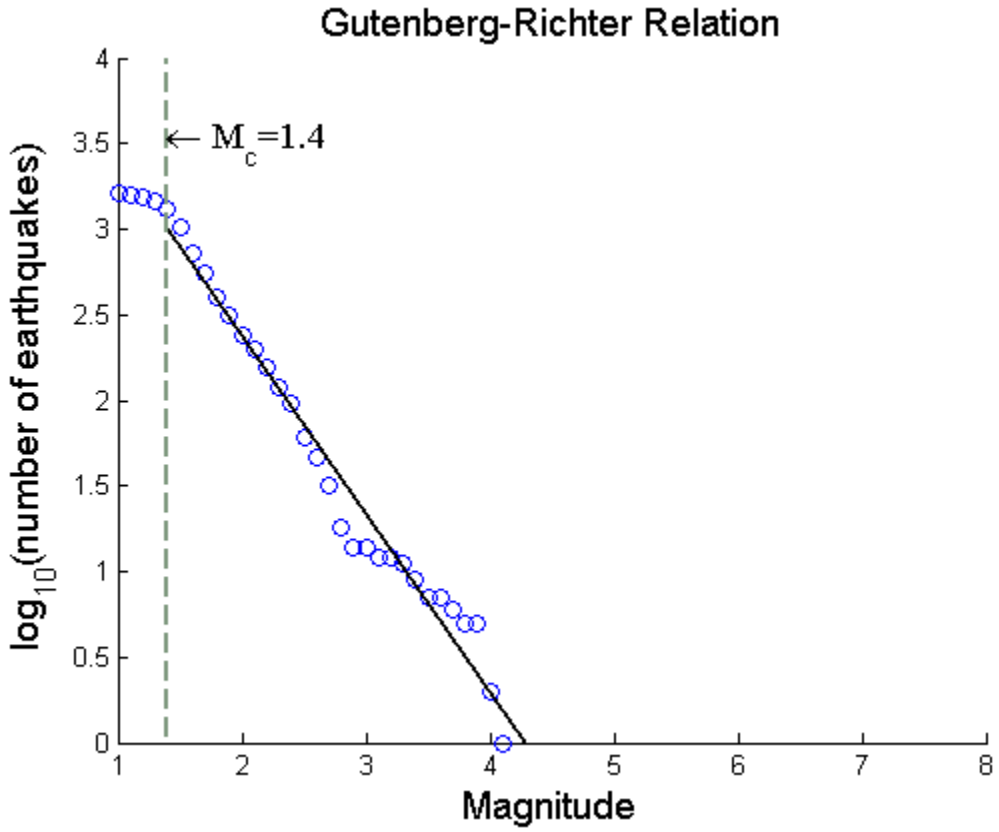

Figure 10. Gutenberg-Richter Relation of the New Madrid Seismic Zone with a magnitude of completeness of $M_C = 1.4$.

In the Gutenberg-Richter plot (Figure 10), the magnitude of completeness is around $M_C = 1.4$. Earthquakes smaller than $M_w = 1.4$ are not detected systematically. Therefore they are included in the catalogue. The dataset collected from CERI contains more than 1660 events over the eight years, which provides a representation of the pre-Mineral activity over eight years. The *b* value forms a linear fit over the $1.4 \leq M \leq 4.1$ ranges. To examine the changes in seismicity rate, all magnitudes below $M_w = 1.4$ were cut out of the catalogue.

Moving Time Window

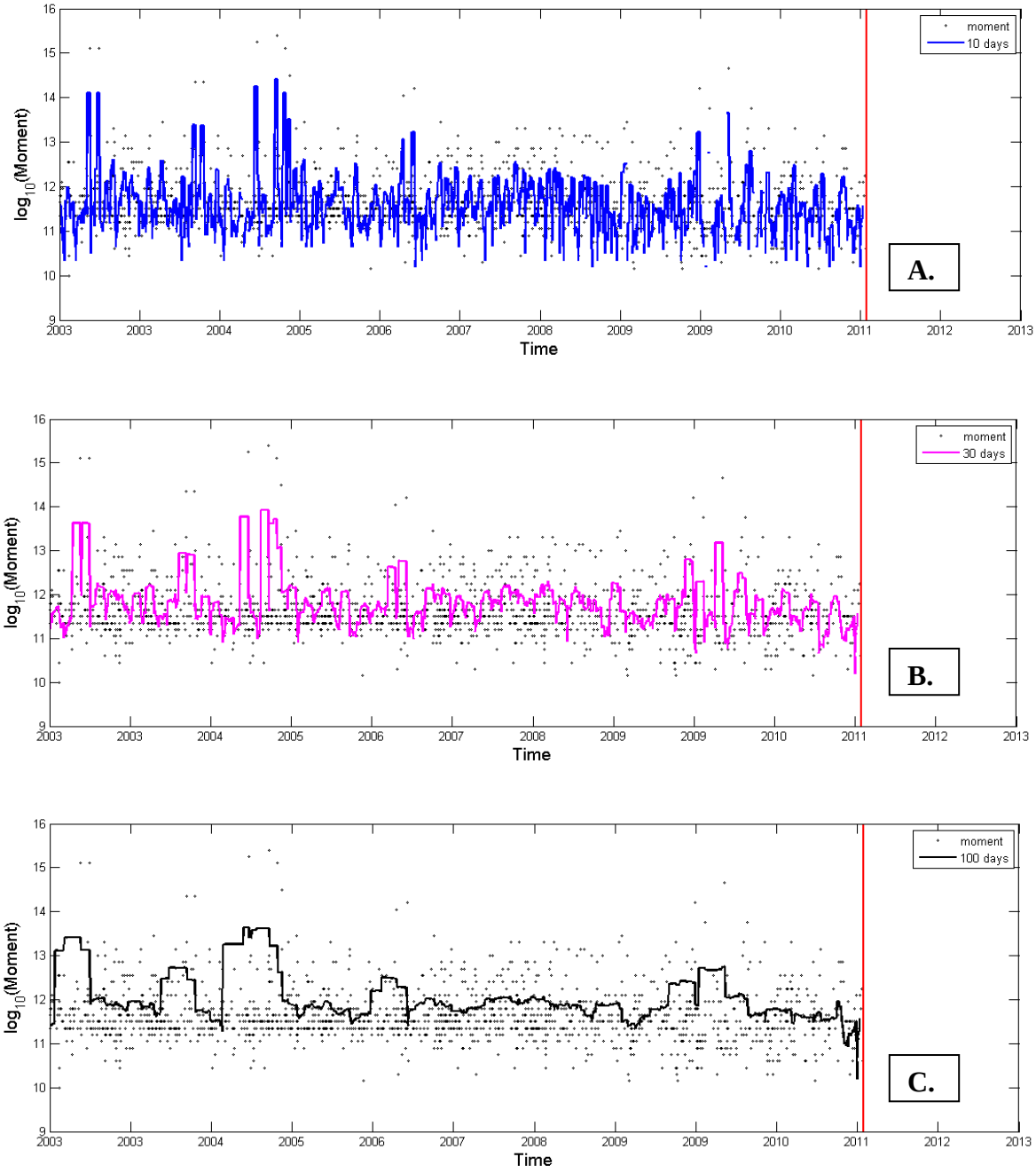

Figure 11. Seismic Moments and window moving averages in an eight year duration of the New Madrid Seismic Zone prior to the Mineral, Virginia event. The red line denotes the break before the Mineral event. **A.** is the 10 day moving time window. **B.** is the 30 day time window. **C.** is the 100 day time window.

The 10 day, 30 day, and 100 day moving window averages were calculated and plotted within the time series (Figure 11). The plot shows seismic moments and the window moving averages in the ten year duration before the Mineral event. The time series are very noisy for the 10 day and 30 day average. The 100 day average is dominated by the occasional large

earthquakes. The New Madrid seismic moments are 100 times smaller than the Mineral event seismic moments.

Cumulative Histogram

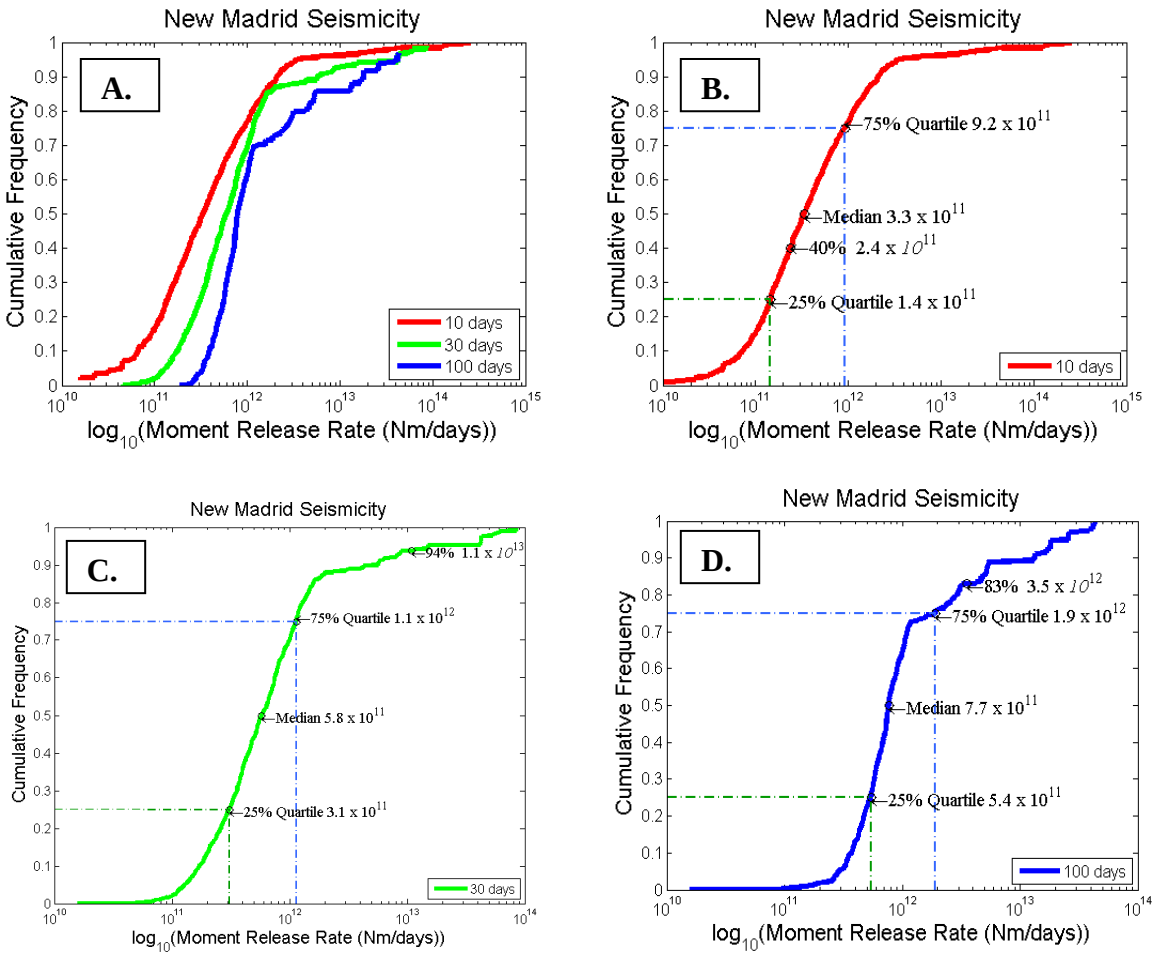

Figure 12. Cumulative Histograms of the New Madrid Seismic Zone before the Mineral Event with the New Madrid results after the Mineral event extracted in three individual times. **A.** shows all of the MRR associated with the window sizes before separating them. **B.** shows the 10 day MRR with the inter-quartile range and the New Madrid results in the post-Mineral event. **C.** shows the similarity with figure B on a 30 day MRR. **D.** shows the similarity with figure B and C on a 100 day MRR.

The cumulative histogram shows the distribution of MRR during the 8 years preceding the Mineral earthquake (Figure 12). The inter-quartile ranges for each of the moving time window averages of the New Madrid in the eight years duration before the Mineral event are reported on the cumulative histograms (Figure 12) and on Table 2. All of the plots show that the MRR in the 75th percentile was three times greater than the median and the median was two times greater than the 25th percentile. The data is skewed towards the larger MRR. The New Madrid MRR after the Mineral event was calculated and presented along with the results before the Mineral event to show if the post results exceed the 95%.

The New Madrid MRR after the Mineral event did not exceed 95%. The 10 day MRR was $2.4x10^{11}$ Nm/Days (41% percentile), the 30 day MRR was $2.44x10^{11}$ Nm/Days (28% percentile), and the 100 day MRR was $3.5x10^{12}$ Nm/Days (83% percentile).

MRR were also calculated with other window sizes ranging from 20 days to 90 days in order to determine whether the Mineral earthquake have an effect in the New Madrid seismicities at different times. The New Madrid results after the Mineral event showed a jump within 30 days and then a steady decay afterwards in the 100 day period. The origin of the jump at 30 days was investigated and it was found that there was a seismic event that occurred in the southern region of Missouri, near Arkansas on September 22, 2011 with a magnitude of M_w=3.6. This seismic event was removed from the post-Mineral New Madrid catalogue. MRR was recalculated to examine if this event has an effect on the seismicity rates of 30 days after the Mineral event. The results are displayed in Figure 13 and Table 2.

Table 2. New Madrid Seismicity Comparison of moment release rates (Nm/Days)

New Madrid Seismic Zone							
	1st Quartile (Nm/Days)	**Median (Nm/Days)**	**3rd Quartile (Nm/Days)**	**Post-Mineral (Nm/Days)**	**Post-Mineral (%)**	**Post-Mineral one event removed (Nm/Days)**	**Post-Mineral one event removed (%)**
10 Days	$1.4x10^{11}$	$3.3x10^{11}$	$9.2x10^{11}$	$2.4x10^{11}$	41%	$2.4x10^{11}$	41%
20 Days	$2.3x10^{11}$	$5.1x10^{11}$	$1.0x10^{12}$	$2.4x10^{11}$	28%	$2.4x10^{11}$	28%
30 Days	$3.1x10^{11}$	$5.8x10^{11}$	$1.1x10^{12}$	$1.1x10^{13}$	94%	$3.8x10^{11}$	33%
40 Days	$3.5x10^{11}$	$6.5x10^{11}$	$1.14x10^{12}$	$8.4x10^{12}$	92%	$4.6x10^{11}$	35%
50 Days	$4.2x10^{11}$	$6.9x10^{11}$	$1.15x10^{12}$	$6.7x10^{12}$	90%	$3.9x10^{11}$	24%
60 Days	$4.5x10^{11}$	$7.2x10^{11}$	$1.13x10^{12}$	$5.7x10^{12}$	89%	$3.8x10^{11}$	19%
70 Days	$4.7x10^{11}$	$7.4x10^{11}$	$1.2x10^{12}$	$4.9x10^{12}$	87%	$3.4x10^{11}$	12%
80 Days	$4.9x10^{11}$	$7.76x10^{11}$	$1.3x10^{12}$	$4.4x10^{12}$	86%	$4.1x10^{11}$	17%
90 Days	$5.1x10^{11}$	$7.7x10^{11}$	$1.4x10^{12}$	$3.9x10^{12}$	84%	$3.9x10^{11}$	14%
100 Days	$5.4x10^{11}$	$7.7x10^{11}$	$1.9x10^{12}$	$3.5x10^{12}$	83%	$3.7x10^{11}$	11%

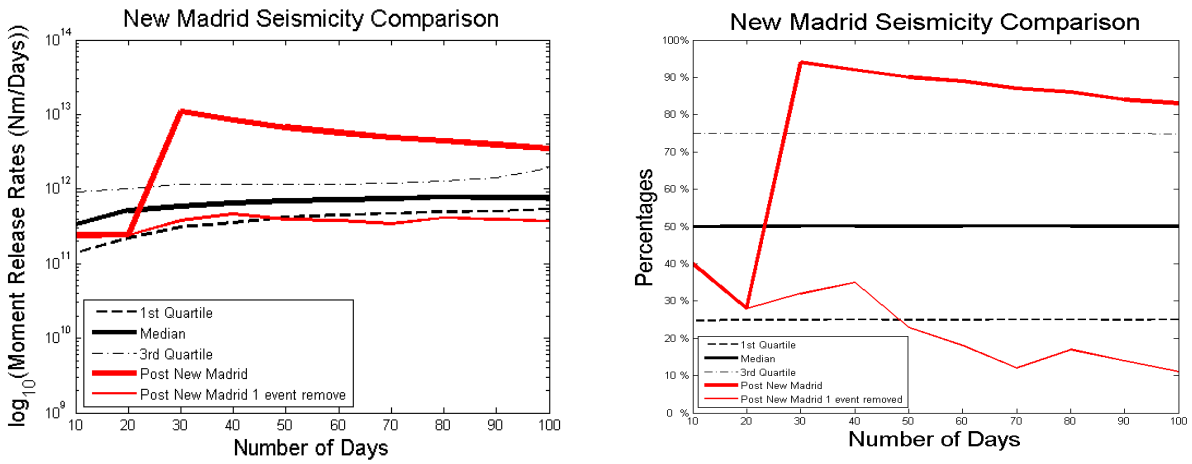

Figure 13. Two plots showing the New Madrid before the Mineral Event data over the inter-quartile range on a 100 day period. **A.** Plot shows the log of the MRR versus the 100 day length of time to express the variability in the data of the large seismic event. **B.** Percentages of the New Madrid after the Mineral Event data over the 100 day length of time to express the variability in the data of the one seismic event.

In figure 13 the plots shows the seismicity comparisons of the New Madrid after the Mineral event with and without the September 22, 2011 seismic event (M_w = 3.6) in red color. The black lines on both plots indicate the inter-quartile ranges. The red line on both plots shows the post-Mineral New Madrid results. The heavy red line includes the M_w = 3.6 event and presents a jump at 30 day which later shows a steady decrease. The thin red line that has the M_w = 3.6 event removed shows variability over the 100 day period.

Removing the September 22, 2011 event (M_w=3.6) removes the sudden jump in seismic release rate after the 30 days. The CERI catalogue after the Mineral event with the seismic event removed showed variability over the 100 day period following the Mineral earthquake (Figure 13A). However, the percentile corresponding to this MRR decreases progressively, showing that the CERI data before the Mineral event is dominated by an occasional large event such as the September 22, 2011 event. There is no evidence that these large events or any of the CERI activity is incompatible with the expectations from the activity before the Mineral event.

Two analyses were conducted to determine how frequently large magnitudes events would be expected to occur. The first analysis was using the Gutenberg-Richter plot to draw how often a seismic event of magnitude M_w=3.6 or larger would occur in a year and when would that next seismic event be expected to occur. The Gutenberg-Richter plot indicates that 5.0 earthquakes of Magnitude M_w=3.6 or larger event took place during the eight years of the catalogue. Therefore, 0.63 earthquakes of magnitude of M_w=3.6 are expected to occur in a year, or equivalently one earthquake every 1.6 years (19 months, or 584 days). The September 22nd event took place 569 days after the previous magnitude $\geq$ 3.5, which appears to be on time. However, this analysis does not take into consideration the natural variability of seismic activity.

The second analysis uses a compilation of the time intervals separating successive large earthquakes over the approximately ten year period from January 01, 2001 to the Mineral event to assess the variability of occurrence of these large earthquakes. For this analysis, a large earthquake is defined as having a magnitude in excess of M_w=3.5. Within that time range, there were 9 seismic events with magnitudes $\geq$ 3.5. The eight time intervals before the Mineral event

were sorted from least to greatest and plotted as a cumulative frequency diagram (Figure 14). The frequencies of the earthquake magnitudes $M_w \geq 3.5$ are spread out due to long time intervals. A statistical analysis was performed and the result was the 75th percentile was five times greater than the median, and the median was two times the 25th percentile. The time interval preceding the September 22, 2011 event was compared to this cumulative frequency diagram to determine how likely it is that these events occurred on that day based on the pre-Mineral activity red star on (Figure 14). The time interval for the post-Mineral event began on March 02, 2010 (M_w=3.7) and ended on September 22nd, 2011 (569 days). The time interval before the September 22, 2011 event is longer than 88% of the pre-Mineral interval. Therefore, there is no indication that this event was exceptionally late (outside to the 1st and 3rd quartile of the pre-Mineral distribution). Figure (**14**) expresses the cumulative frequency on the y-axis and the number of days on the x-axis.

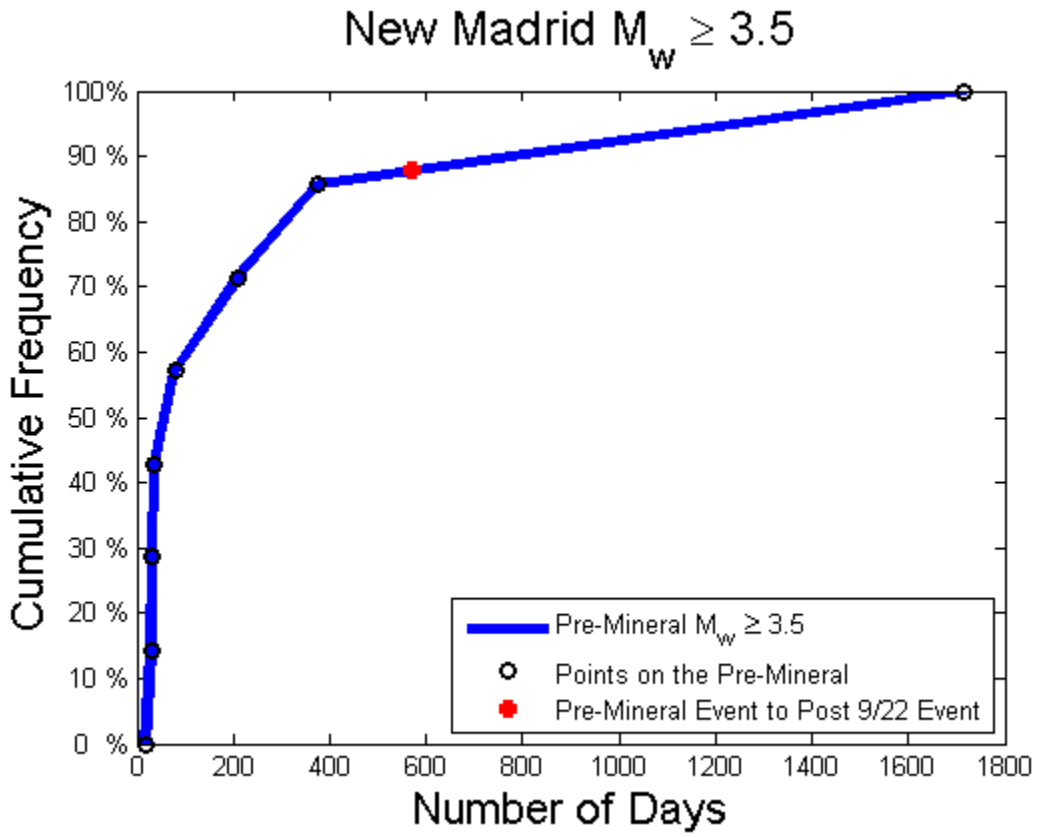

Figure 14. Plot of New Madrid seismicity with $M_w \geq 3.5$ over a 10 year period.

Discussions

Though intraplate earthquakes are known to be rare, they are widely felt, large, and damaging. The implications from intraplate earthquakes have an effect on mortality, economy, and damage to the infrastructure. The Charleston earthquake in 1886 killed over 60 people and cost $6 million in property damage (USGS, 2012). The Mineral earthquake caused extensive damage to the National Cathedral and Washington Monument which is still closed to the public and currently undergoing repairs (Figure 2b) (Horton et al, 2012).

In densely populated metropolitan regions that contain tall buildings and nuclear reactors, such as Washington D.C., earthquakes have the possibility to increase the mortality rate and cause extensive property loss. Education can be promoted by the need to understand the seismic hazards in intraplate regions.

The Indian Ocean earthquake M_w= 8.6 that occurred on April 11, 2012 is by far the largest strike-slip event ever to be recorded. This large strike-slip event reached remote distances of 10,000 km to 20,000 km from the epicenter (Pollitz et al, 2012). The Indian Ocean event triggered aftershocks for six days afterwards with magnitudes ≥ 5.5 at almost five times the normal rate all around the world (Pollitz et al, 2012). These global aftershocks were located along the four lobes of Love-wave radiation (Pollitz et al, 2012). Generally, aftershocks are restricted to the immediate vicinity of a main shock; the Indian Ocean event challenges us to study how soon and how close aftershocks can occur to large earthquakes.

The August 23, 2011 Mineral, Virginia earthquake M_w= 5.8 was the largest reverse fault slip event ever to be recorded in the Central-Eastern United States since 1897 (Jibson and Harp, 2012). Like the Indian Ocean event, the Mineral earthquake was broadly felt over the eastern United States. However the triggered aftershocks were restricted to the vicinity of Mineral, Virginia and did not have magnitudes at abnormally high rates. The triggered aftershocks decayed over a short period of time and were not felt broadly across the Central-Eastern United States. One way to investigate this matter was by examining the New Madrid Seismic region to observe if the Mineral event had an effect on the seismicity in this area. The statistical methods used for the Mineral event were applied to the New Madrid region. The results revealed that the Mineral event had no effect on the seismicity in the New Madrid Seismic Zone. Though the Indian Ocean earthquake and the Mineral earthquake were the largest earthquakes to be recorded and broadly felt in their respective regions, the Indian Ocean earthquake had a larger magnitude and completely different focal mechanism than the Mineral earthquake.

Conclusion

The examination of seismicity rate changes in the August 23, 2011 Mineral earthquake reveals the conclusion that the moment release rates without the aftershocks in the Central Eastern US did not exceed the 95th percentile confidence level. Therefore the magnitudes in the Central Eastern US have not increased after the Mineral earthquake.

This method from the IRIS analysis was similarly applied to another intraplate region which was the New Madrid Seismic Zone. The observation of seismicity rate changes in the New Madrid Seismic Zone reveals that the moment release rates after the Mineral event did not exceed the 95% confidence level. Therefore the magnitudes in the New Madrid Seismic Zone have not increased nor has it been affected by the August 23, 2011 Mineral earthquake event.

Acknowledgements

I would like to thank my advisor Dr. Laurent Montési for his guidance through the research and writing of this thesis. I would also like to thank Dr. Lisa Walsh and Dr. Lekic for their comments and assistance to me in my thesis project and to all the undergraduate and graduate students in the geology department.

Bibliography

Fenster, D. F., and L. S. Walsh (2011), Preliminary information on the Mw 5.8 Mineral, VA, earthquake, AEG News, 54(4), 26–30.

Freed, A.M., and Lin, J. (2001), Delayed triggering of the 1999 Hector Mine earthquake by viscoelastic stress transfer, Nature 411, 180-183.

Horton, J.W. and Williams, R.A. (2012), The 2011 Virginia Earthquake: What Are Scientists Learning? EOS, Trans. Am. Geophys. U., 92, p.317-324, doi: 10.1029/2012EO330001

Hough, S. E. (2012), Initial assessment of the intensity distribution of the 2011 Mw 5.8 Mineral, Virginia earthquake, Seismol. Res. Lett., 83(4), 649-657, doi:10.1785/0220110140.

Jibson, R.W., and Harp, E.L. (2012), Extraordinary distance limits of landslides triggered by the 2011 Mineral, Virginia, earthquake, Bull. Seismol. Soc. Am. 102(6), 2368-2377, doi:10.1785/012010055.

Kilb, D., Gomberg, J., and Bodin, P. (2000), Triggering of earthquake aftershocks by dynamic stresses. Nature 408, 570–574.

McNamara, D.E., R. Herrmann, H. Benz, A. Leeds, M. Chapman, and L. Gee (2013), The Mw 5.8 Mineral, Virginia earthquake of August 23, 2011 and aftershock sequence: Constraints on earthquake source parameters and fault geometry, edited, *Bulletin of the Seismological Society of America*, in review.

Pollitz, F.F., Stein, R.S., Selvigen, V., and Bürgmann, R. (2012), The 11 April 2012 east Indian Ocean earthquake triggered large aftershocks worldwide, Nature 490, 250-253, doi:10.1038/nature11504

Stein, R.S. (1999), The role of stress transfer in earthquake occurrence, Nature 402, 605-609.

Stein, R.S. (2010), *Disasters Deferred. How new science is changing our view of earthquake hazards in the Midwest.* Columbia University Press, New York, NY.

USGS (2012), "Historic Earthquakes New Madrid 1811-1812" Historic Earthquakes. 01 Nov. 2012. United States Geological Survey. 05 Nov. 2013 <http://earthquake.usgs.gov/earthquakes/states/events/1811-1812.php>.

USGS (2012), "Historic Earthquakes Charleston." Historic Earthquakes. 01 Nov. 2012. United States Geological Survey. 05 Nov. 2013 <http://earthquake.usgs.gov/earthquakes/states/events/1886_09_01.php>

Velasco, A. A., Hernandez, S., Parsons, T. & Pankow, K. (2008), Global ubiquity of dynamic earthquake triggering. Nature Geosci. 1, 375–379

Appendix A

Mineral, Virginia Event aftershocks reported from the USGS web Browser

Mineral, Virginia Aftershocks reported from USGS					
Date	**Time (UTC)**	**Latitude**	**Longitude**	**Depth (km)**	**Magnitude**
23-Aug-11	17:51	37.936	77.933	6	5.8
23-Aug-11	18:46	37.931	77.935	0.1	2.8
23-Aug-11	19:20	37.911	78.004	0.1	2.2
24-Aug-11	0:04	37.925	77.951	7.9	4.2
24-Aug-11	4:45	37.925	77.994	4.9	3.4
25-Aug-11	4:06	37.923	77.988	0.1	2.5
25-Aug-11	5:07	37.94	77.896	5	4.5
25-Aug-11	6:37	37.912	77.969	0.1	2.3
25-Aug-11	15:27	37.951	77.924	0.1	2.4
25-Aug-11	23:40	37.903	77.814	4.9	2.6
26-Aug-11	22:52	37.888	77.939	0.1	2.1
27-Aug-11	9:02	37.925	77.977	0.1	2
28-Aug-11	20:18	37.933	77.969	6.7	2.2
29-Aug-11	1:06	37.933	77.987	4.6	2.3
29-Aug-11	3:15	37.971	78.024	5.8	2
29-Aug-11	3:16	37.938	78.006	5.1	2.7
29-Aug-11	4:19	37.901	77.901	5	2.2
30-Aug-11	3:48	37.907	77.976	7.2	2.6
30-Aug-11	13:26	37.92	77.978	5.8	2.1
31-Aug-11	13:44	37.922	77.882	0.7	2.1
31-Aug-11	15:01	37.953	77.977	3.6	1.8
1-Sep-11	9:09	37.958	77.882	4.9	3.4
16-Sep-11	16:17	37.937	77.987	4.6	2.1
17-Sep-11	8:33	37.928	77.988	5.1	2
17-Sep-11	12:42	37.942	77.978	5.1	1.9
17-Sep-11	15:33	37.925	77.987	4.8	2.6
17-Sep-11	18:37	37.974	77.827	3.2	2.1
18-Sep-11	8:43	37.952	77.942	3.2	2.1
19-Sep-11	4:58	37.977	77.831	2.6	2
19-Sep-11	15:29	37.915	78.002	3.3	1.8
19-Sep-11	20:33	37.976	77.829	3	2.3

(Source: USGS)

Appendix B. Parsing the IRIS catalogue in Matlab

```
function seis=ReadWeed(fname)
% Read weed files obtained from IRIS
% Convert magnitude to moment (SI units)
% Convert date to universal date using Matlab's datenum
%%%%%%%%%%%%%%%%%%%%%%%%%%%%%%%%%%%%%%%%%%%%%%%%%%%%%%%%%%%%%%%%%%%%%%%%%%%%
% seis: storage structure for database
%      .filename  : name of the original weed file
%      .cat       : name of the catalogue
%      .date      : date for each event
%      .datenumber: Matlab datenumber for each event
%      .time      : Time for each event (includes hour, minute, second)
%      .lat       : Latitude for each event
%      .long      : Longitude for each event
%      .depth     : Depth for each event
%      .magtype   : Type of magnitude for each event
%      .mag       : Magnitude for each event
%      .moment    : Moment of each event
%      .n         : Number of events
%      .gr        : Guntenberg-Richter analysis (done by seismicity.m)
%            .Mall     : Magnitude bins
%            .c        : Cum. number of moments with mag. larger than Mall
%            .fit      : Structural array with fields p and bounds
%      .movav     : Moving Window averages for Time Series Plot
%            .Window size : Number of moving window averages
%            .Start    :Structural array bookcase that includes the
%                       startday, endday,mosum, morate, moq, q
%                .Startday : Day of Start day
%                .Mosum    : Sum of the Moments
%                .Morate   : Moment Release Rates
%                .Moq      : Seismic Moments of q
%                .q        : Number of each seismic event in the catalogue
%                .endday   : Day of End day
%
% Parsing weed file
[cat,date,time,lat,long,depth,scrapone,scraptwo,magtype,mag]=...
    textread(fname,'%[^,] , %s %[^,] , %f, %f, %f, %[^,], %[^,], %[^,] , %f');
% Calculate seismic moment
moment=10.^(((3/2)*mag) + 9.1);
% Time Series
datenumber=datenum(date);
% Store information into seis
seis.filename=fname; %name of original weed file
seis.cat=cat; % name of catalogue
seis.date=date;
seis.datenumber=datenumber;
seis.time=time; %time of event
seis.lat=lat; %lat coordinates of event
seis.long=long; %long coordinates of event
seis.depth=depth; %depth of event
seis.magtype=magtype; %magtype of event
seis.mag=mag; %mag of event
seis.moment=moment; %seismic moment
seis.n=numel(cat); %number of events in catalogue
end
```

Appendix C. Matlab Script for Seismicity in computing the Gutenberg-Richter Relation

```
% Gutenburg Richter relation
Mall=[1.0: 0.1: 6.0];
c=[  ];
mag=seis.mag;
for i= 1:numel(Mall)
        c(i)=sum(mag > Mall(i));
end
seis.gr.Mall=Mall; %Magnitude values for Gutenberg-Richter plot
seis.gr.c=c; % cumulative number of moments with magnitude larger than Mall
lc=log10(c);
ic=0; interval=0.1;
for m1=1:interval:(5-interval);
    for m2=(m1+interval):interval:5;
        ic=ic+1;
        im=find((Mall>=m1)&(Mall<=m2)&(c~=0));
        if numel(im)>=2;
        seis.gr.fit(ic).p=polyfit(Mall(im),lc(im),1);
        else
            seis.gr.fit(ic).p=[NaN,NaN];
        end
        seis.gr.fit(ic).bounds=[m1,m2];
    end
end
```

Plotting the Gutenberg-Richter Relation

```
function plotgrs(seis,Mbounds)
Mall=seis.gr.Mall; %Magnitude values for Gutenberg-Richter plot
lc=log10(seis.gr.c); % cumulative number of moments with magnitude larger than
Mall
% Gutenberg-Richter plot
figure(1);
clf;
hold on;
plot(Mall,lc,'o')
xlim([1 8]);ylim([0,4]);
xlabel('Magnitude');
ylabel('log10(Number of Earthquakes)');
title('Gutenberg-Richter Relation');

msort=reshape([seis.gr.fit.bounds],[2,numel(seis.gr.fit)]);
ib=find((msort(1,:)==Mbounds(1))&(msort(2,:)==Mbounds(2)));
f=polyval(seis.gr.fit(ib).p,Mbounds);
figure(1);
plot(Mbounds,f,'-k','linewidth',2)
pall=reshape([seis.gr.fit.p],[2,numel(seis.gr.fit)]);
mdiff=msort(2,:)-msort(1,:);
figure(2);
im=find(mdiff>=1);
plot(msort(1,im),pall(1,im),'co'); xlabel('Magnitude');
```

Appendix D. Matlab Script for computing the Moving Time Window

```
function seis=movingwindowaverage(seis,windowall);
moment=seis.moment;
iw=0; moq=0; morate=0; mosum=0;q=0;
for windowsize=windowall;
    iw=iw+1;    is=0;
   daymin=min(seis.datenumber);
   daymax=max(seis.datenumber);
   startlist=daymin:daymax-windowsize;

    for startday=startlist;
        is=is+1;
               endday=startday+windowsize;
               q=find((seis.datenumber>=startday)&(seis.datenumber<endday)...
                   &(seis.mag<=8.0)&(seis.mag>=3.5));
                   moq=moment(q);
                mosum=sum(moq);
                morate=mosum./windowsize;

        seis.movav(iw).windowsize=windowsize;
        seis.movav(iw).start(is).mosum=mosum; % Sum of the Moments
        seis.movav(iw).start(is).morate=morate; % Moment Release Rates
        seis.movav(iw).start(is).moq=moq; % Seismic Moment of q
        seis.movav(iw).start(is).q=q;   % No. of each seismic event in the
catalogue
        seis.movav(iw).start(is).startday=startday; %Day of Start Day
        seis.movav(iw).start(is).endday=endday; %Day of End Day
    end

end
```

Plotting the Moving Time Window

```
date=seis.date;
datenumber=datenum(date);
startDate=datenum('01-01-2001');endDate=datenum('01-16-2013');
moment=seis.moment;
xData=linspace(startDate,endDate,13);
plot(datenumber, log10(moment),'ko','markerfacecolor',[0.6 0.6
0.6],'markersize',2);ylim([10 18]);
xlabel('Time','FontSize',14);ylabel('log_{10}(Moment)','FontSize',14);
set(s(1),'XTick',xData);
datetick(s(1),'x','yyyy','keepticks');
hold on
colr{1}='k' ;colr{2}='m';colr{3}='k';
for iw=1:size(seis.movav,2)
for n=1:length(seis.movav(iw).start)
    startday(n)=seis.movav(iw).start(n).startday;
    morate(n)=seis.movav(iw).start(n).morate;
end
plot(startday,log10(morate),colr{iw},'linewidth',2);
hleg1=legend('moment','10 days','30 days','100 days');
end
hold on
plot([1,1]*datenum('23-Aug-2011'),[10,18],'r','linewidth',2);
```

Appendix E. Matlab Script for the computing and plotting the Cumulative Histogram

```
colr{1}='r';colr{2}='g';colr{3}='b';
colr{4}='m';colr{5}='c';colr{6}='k';colr{7}='y';
ncol=numel(colr);

figure(1);clf;hold on;
%% Moment Release Rate Plot
    for ir=1:numel(seis.movav)
        for z = 1:length(seis.movav(ir).start)
            info1(z) = seis.movav(ir).start(z).morate;
        end
%% Cumulative Frequency Plot
B=sort(info1);
ya=linspace(0,1,numel(info1));
plot(B,ya,colr{1+mod(ir-1,ncol)},'linewidth',2);

%% Statistical Analysis
M=median(B);
Q1=median(B(find(B<median(B)))); % 25%
Q3=median(B(find(B>median(B)))); % 75%
plot(M,0.5,'ko');hold on;plot(Q1,0.25,'ko');hold on;plot(Q3,0.75,'ko');
%% Percentages
% With Aftershocks
mrr1=3.9e13;
ind1=find(B>=mrr1, 1);
mrra1=ya(ind1)
% Without Aftershocks
mrr2=1.2e14;
ind2=find(B>=mrr2,1);
mrra2=ya(ind2)
%%
% hold on; plot(1.7e+14,0.558,'ko'); % Post Mineral with aftershock
% hold on; plot(1.3e+14,0.52686,'ko'); % Post Mineral without aftershock
end
%% Add ons
hleg1=legend('10 days','30 days','100 days',4);
set(gca,'fontsize',12);
title('Pre-Mineral Event Cumulative Histogram'); xlabel('log_{10}(Moment
Release Rate (Nm/Days))','FontSize',16); ylabel('Cumulative
Frequency','FontSize',16);
set(gca,'xscale','log');box on;
```

Appendix F

Honor Code

I pledge on my honor that I have not given or received any unauthorized assistance or plagiarized on the assignment.

X_____